Biochemistry and Biophysics Reports 5 (2016) 296–304

Contents lists available at ScienceDirect

Biochemistry and Biophysics Reports

journal homepage: www.elsevier.com/locate/bbrep

A novel SOD mimic with a redox-modulating mn (II) complex, ML1 attenuates high glucose-induced abnormalities in intracellular Ca^{2+} transients and prevents cardiac cell death through restoration of mitochondrial function

Vasundhara Kain [a,1], Mithila A. Sawant [a,2], Aparajita Dasgupta [a,2], Gaurav Jaiswal [a,3], Alok Vyas [b,4], Subhash Padhye [b], Sandhya L. Sitasawad [a,*]

[a] National Centre for Cell Science, S.P. Pune University Campus, Ganeshkhind Road, Pune 411007, Maharashtra, India
[b] ISTRA, Department of Chemistry, Abeda Inamdar Senior College, University of Pune, Pune 411001, India

ARTICLE INFO

Article history:
Received 27 July 2015
Received in revised form
25 December 2015
Accepted 7 January 2016
Available online 8 January 2016

Keywords:
Mn-Superoxide dismutase
Mitochondrial superoxide
Diabetic cardiomyopathy
Hyperglycemia
ARVM
Cardiomyocytes

ABSTRACT

A key contributor to the pathophysiology of diabetic cardiomyopathy, mitochondrial superoxide can be adequately countered by Mn-superoxide dismutase, which constitutes the first line of defense against mitochondrial oxidative stress. Our group has recently synthesized low molecular weight SOD mimics, demonstrating superior protection against oxidative damages to kidney cells. In the current study, we sought to evaluate the protective effect of the SOD mimic ML1 against high glucose induced cardiomyopathy in diabetes. Mechanistic studies using rat cardiac myoblast H9c2 showed that ML1 markedly inhibited High Glucose (HG) induced cytotoxicity. This was associated with increased Mn-SOD expression along with decreased mitochondrial O_2^-, ONOO- and Ca^{2+} accumulation, unveiling its anti-oxidant potentials. ML1 also attenuated HG-induced loss of mitochondrial membrane potential ($\Delta\Psi_m$) and release of cytochrome c, suggesting that ML1 effectuates its cytoprotective action via the preservation of mitochondrial function. In an ex-vivo model normal adult rat ventricular myocytes (ARVMs) were isolated and cultured in either normal glucose (5.5 mmol/l glucose) or HG (25.5 mmol/l glucose) conditions and the efficiency of ML-1 was analyzed by studying contractile function and calcium indices. Mechanical properties were assessed using a high-speed video-edge detection system, and intracellular Ca^{2+} transients were recorded in fura-2–loaded myocytes. Pretreatment of myocytes with ML1 (10 nM) ameliorated HG induced abnormalities in relaxation including depressed peak shortening, prolonged time to 90% relenghthening, and slower Ca^{2+} transient decay. Thus, ML1 exhibits significant cardio protection against oxidative damage, perhaps through its potent antioxidant action via activation of Mn-SOD.

1. Introduction

Diabetic cardiomyopathy remains the most debilitating and challenging feature of diabetes progression. Hyperglycemia, a hallmark of diabetes is known to be intimately associated with ventricular dysfunction that can lead to severe cardiac impairment and cell death [1–5]. Currently available pharmacological measures for managing hyperglycemia are principally designed around achieving strict blood glucose control in diabetic patients. Although these approaches slow down the progression of cardiac damage, they fail to ultimately prevent the development of cardiomyopathy (DCM). Thus, additional strategies to protect the heart against diabetes-induced cardiac dysfunction are required.

Hyperglycemia results in the generation of Oxidative stress, induced by superoxide generation (O_2^-) and, associated nitrosative damage, which contribute indisputably to disease progression culminating in DCM [6,7]. Mitochondria are the major source of reactive oxygen species (ROS) and Mitochondrial oxidative stress has been implicated to be primarily responsible for these deleterious effects [8–12]. Hence, novel approaches to block excessive O_2^- generation in diabetic mitochondria may offer a therapeutic benefit by preventing the development of DCM. Superoxide dismutase (SOD) is an endogenous anti-oxidant, which combats

* Corresponding author.
E-mail address: ssitaswad@nccs.res.in (S.L. Sitasawad).
[1] Present address: Division of Cardiovascular Disease, Department of Medicine, The University of Alabama at Birmingham Birmingham, Alabama, USA.
[2] Both authors contributed equally to the work.
[3] Present address: Scientific Officer, PanEra Biotec. Pvt Ltd., Lalru, Mohali, Punjab, India
[4] Present address: Crest Premedia Ltd., Upper Ground Floor, Wing B, Tower–8, Magarpatta City SEZ Hadapsar, Pune 411013, Maharashtra, India.

http://dx.doi.org/10.1016/j.bbrep.2016.01.003
2405-5808/

oxidative stress under physiological and pathological conditions. Therefore, the development of therapeutics aimed at mimicking SOD could provide tactical advantage.

Small molecular weight, manganese porphyrins have been shown to be of great therapeutic value in a variety of disease processes, including diabetes [13], myocardial ischemia–reperfusion injury [14], dilated cardiomyopathy [15], amyotrophic lateral sclerosis (ALS) [16], retinal injury [17] and epilepsy [18]. The protective effects of manganese porphyrins have been attributed to their antioxidant properties, including SOD-mimicking and radical scavenging activity [19–21]. In addition, the manganese porphyrins are cell permeable, making it possible to provide both intracellular and extracellular protection against oxidative stress. In our previous study, we have demonstrated that certain novel synthetic manganese complexes of α-heterocyclicthiosemicarbazone ligands show superior protection against oxidative damages to Hek293 kidney cells. These complexes mimic the structural features of the core motif of Mn-SOD [22]. In the current study, we evaluated the protective effects of one of these Mn-SOD mimetics ML-1, against diastolic dysfunction in DCM. We demonstrate that this compound exhibits significantly enhanced protection against high glucose injury, presumably due to a combination of anti-oxidative and calcium regulatory mechanisms.

2. Materials and methods

2.1. Chemicals

ML1 is a five co-ordinate ternary manganese complex prepared by employing combination of tri-dentate thiosemicarbazone ligands and bi-dentate bipyridyl/aminoethanethiol as ancillary ligands as previously reported [22]. 3-(4,5-Dimethylthiazol-2-yl)-2,5-diphenyltetrazolium bromide (MTT), 4′,6-diamidino-2-phenylindole (DAPI), dimethyl sulfoxide (DMSO), D-glucose, were purchased from sigma, 9-[4-[bis[2-[(acetyloxy)methoxy]-2-oxoethyl]amino]-3-[2-[2-[bis[2- [(acetyloxy) methoxy]-2 oxoethyl] amino] phenoxy] -ethoxy] phenyl] -3, 6-bis(dimethylamino)-bromide (Rhod 2 AM), MitoSOX red, dihydrorhodamine-123 (DHR-123) 3,3′-dihexyloxacarbocyanine iodide ($DiOC_6$) and Ionomycin were from molecular Probes, Invitrogen. xanthine, xanthine oxidase, calcium chloride, EGTA, mn-SOD and mn-SOD antibody were purchased from sigma-Aldrich (st. louis, MO). PARP antibody was from BD biosciences.

2.2. Cell cultures and treatments

H9c2 cells (ATCC CLR-1446; Rockville, MD) were maintained in Dulbecco's modified Eagle's medium (DMEM) supplemented with 10% fetal bovine serum (FBS) from Gibco, USA. When cell populations reached 40–50% confluence, the cultures were exposed to D-glucose in a final concentration of 33 mM in cultures and was termed high glucose (HG) according to previous publications [1,23] and 5.5 mM concentration was used as normal glucose (NG). Varying concentrations of ML1 were used for the initial experiments (0–100 nM). 0.1 mM Xanthine+0.01 U Xanthine oxidase (X+XO, superoxide generator) and 100U Mn-SOD were used as positive controls. Independently, for various experimental controls, cells were also treated with Calcium (1 μM), calcium chelator EGTA (10 μM) and Ionomycin (5 μg/ml). After exposure for desired time periods, the monolayer cultures were washed with PBS and the cells were removed by trypsinization. In some experiments, the cells were grown on glass coverslips, which were used for calcium, ROS and RNS detection and mitochondrial membrane potential.

2.3. Cell viability

For determination of cell viability, 3.5×10^4 cells/well in a 96-well microplate were incubated in 100 μl of culture media and exposed to 5.5 and 33 mM of glucose with or without various concentrations of ML1 (0–100 nM) and 100U Mn-SOD for varying time periods. 0.1 mM X+0.01U XO (superoxide generator) was used as a positive control. The media were removed again and replaced with 90 μl of DMEM (containing no phenol red or FBS) and 10 μl of MTT solution (2 mg/ml phosphate buffer) for 4 h. After the MTT-containing DMEM was removed, the remaining formazan blue crystals were dissolved in 100 μl of DMSO solution. Absorbance at 570 nm was measured using a microplate reader (Molecular Devices, SpectraMax 250). The cytotoxicity curve was constructed from at least three independent experiments and expressed as percentage cell viability compared to control.

2.4. Mitochondrial superoxide and peroxynitrite generation

Mitochondrial superoxide generation was detected by using a specific mitochondrial superoxide indicator, MitoSOX™ red [24], a modified cationic dihydroethidium. MitoSOX™ red is a cell-permeative dye that reacts with superoxide to form ethidium, which upon binding to nucleic acids gives a bright red fluorescence. Briefly, after 48 h HG treatment, the cells grown on specialized coverslips were loaded with MitoSOX™ red (5 μM; 10 min at 37 °C). Peroxynitrite was measured using DHR 123 (5 μM) [25–27]. After being stained, the cells were washed in PBS and fixed with 10% buffered formalin. Coverslips were mounted on glass slides and observed using a confocal laser-scanning microscope (Zeiss CLSM 510) with a 63X objective. Three fields per image chosen at random, from 3 independently performed experiments were used for quantification.

2.5. Measurement of mitochondrial calcium

Mitochondrial calcium was measured by incubating the cells with 2 μM Rhod-2 AM dye. Briefly, after 48 h HG treatment, the cells, grown on specialized coverslips were loaded with Rhod-2 AM (2 μM; 10 min at 37 °C). After being stained, the cells were washed in PBS and fixed with 10% buffered formalin. Coverslips were mounted on glass slides and observed using a confocal laser-scanning microscope (Zeiss CLSM 510) with a 63X objective. Three fields per image chosen at random, from 3 independently performed experiments were used for quantification.

2.6. Determination of mitochondrial membrane potential ($\Delta\Psi_m$) and assessment of mitochondrial cytochrome c release

The mitochondrial membrane potential ($\Delta\Psi_m$) was assessed using $DiOC_6$ [27,28]. Briefly, H9c2 cells were cultured in six-well plates and treated with 5.5 and 33 mM of glucose with or without ML1 (10 nM) and 100U Mn-SOD for 48 h. Subsequently, cells were loaded with 60 nM $DiOC_6$ for the last 30 min and washed and images were captured using a confocal microscope as described above.

Evaluation of the sub-cellular localization of cytochrome c was done by using confocal imaging of cells double-labeled with MitoTracker™Red (Molecular Probes) and cytochrome c antibody (Cell Signaling) according to previous methods [23]. Briefly, cells treated with NG and HG for 72 h were incubated with 100 nM MitoTracker™ Red, fixed with 3% paraformaldehyde, permeabilized with 0.02% Triton X and blocked with 5% BSA, followed by incubation with primary rabbit polyclonal cytochrome c antibody (1:50) for 2 h at room temperature and Cy2-conjugated goat anti-rabbit antibody (1:500; Chemicon International, Temecula, CA,

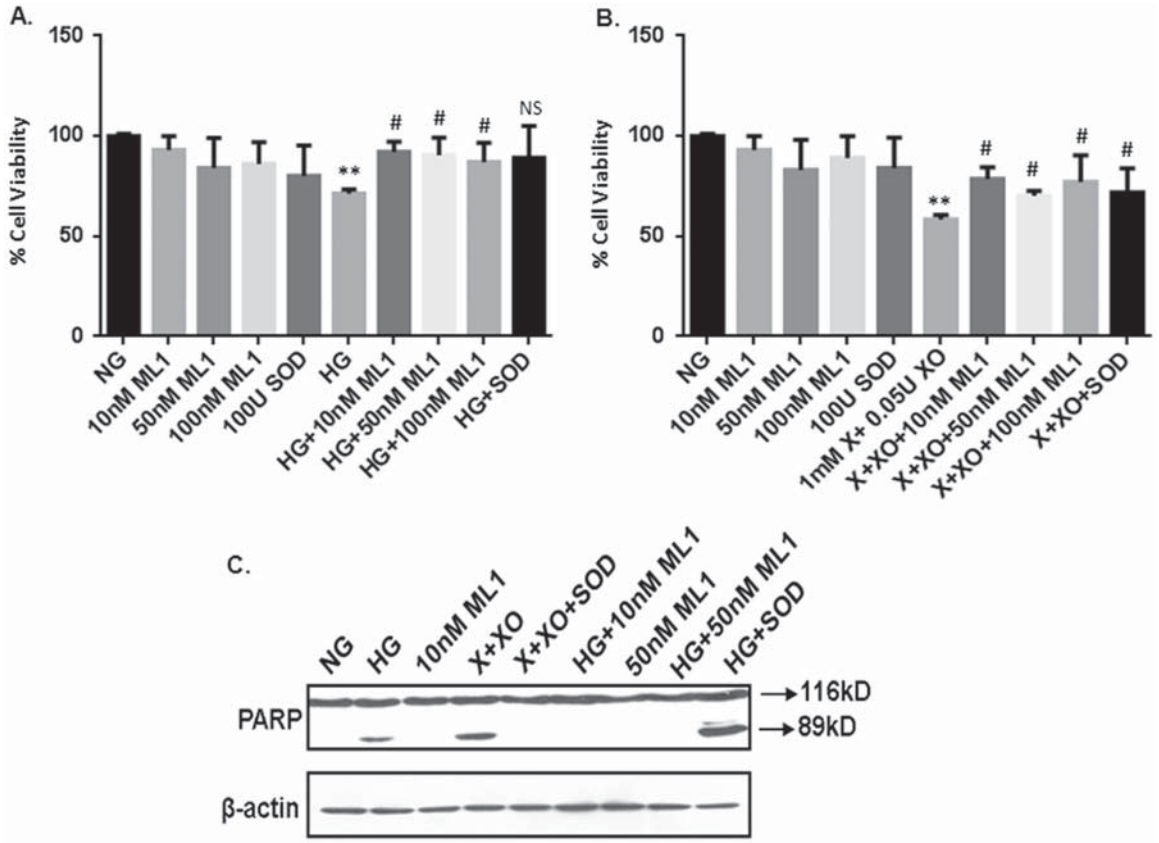

Fig. 1. ML1 prevents cardiomyoblast cell death. (A) Cytoprotective effect of ML1 was assessed using MTT assay against HG induced cell death. NG treated wells were normalized to 100% cell viability. (B) Cytoprotective effect of ML1 was assessed using MTT against oxidative stress induced cell death. X+XO was used as a superoxide generator. Control wells were normalized to 100% cell viability. Columns, mean from three independent experiments performed in triplicate; bars, SE. ns > 0.05 versus NG and HG, $^{**}P < 0.01$ versus NG and $^{\#}P < 0.05$ versus HG or X+XO as appropriate. (C) PARP cleavage was studied by western blotting. β actin was used as loading control. Image representative of three independent experiments.

USA) for 1 h. Coverslips were mounted with antifade on glass slides and images were acquired using a confocal microscope. Untreated unstained cells served as negative control and untreated fluorophores loaded cells served as control for background subtraction for confocal experiments.

2.7. Analysis of Mn-SOD and PARP cleavage

To analyze PARP cleavage [29], and Mn-SOD expression, cells (3.5×10^4) were treated with 5.5 and 33 mM glucose with or without various concentrations of ML1 and 100U Mn-SOD for the indicated time. Cells were scraped into radio-immunoprecipitation assay lysis buffer (120 mM NaCl, 1.0% Triton X-100, 20 mM Tris–HCl, pH 7.5, 10% glycerol, 2 mM EDTA, protease inhibitor cocktail (Roche GmbH, Germany) and the protein concentration in each sample was determined using a Bio-Rad protein assay kit with BSA as the standard. For immunoblotting, 40 μg of protein lysate per sample was denatured in 4 × SDS–PAGE sample buffers and resolved by 8–12% SDS–PAGE, transferred to a PVDF membrane (Millipore, Germany), blocked with nonfat milk, and probed for *PARP*, Mn-SOD using *HRP*-conjugated appropriate secondary antibody. The enhanced chemiluminescence was detected using the Femto chemiluminescence detection system (Pierce Chemical, Rockford, IL, USA). Membranes were stripped and re-probed with *β-actin* (ICN Biomedicals, USA) primary antibody (1:10,000) as a protein loading control. Densitometry was performed using Image J software.

2.8. Isolation and culture of ventricular myocytes

The experimental procedure used in this study was approved by the Institutional Animal Ethical Committee at the National Centre for Cell Science, Pune, India. Adult rat cardiomyocytes were isolated as described previously [3,30]. Isolated myocytes were then treated with 5.5 and 33 mM glucose with or without 10 nM ML1.

2.9. Cell shortening/ re-lengthening and intracellular Ca^{2+} fluorescence measurement in adult cardiomyocytes

The mechanical properties of ventricular myocytes were assessed using a SoftEdge MyoCam system (IonOptix Corp., Milton, MA, USA) [3,30]. After 24 h treatment of cells with HG, cell shortening and relenghthening were assessed using the following indices: peak shortening (PS)—indicative of peak ventricular contractility, time to PS (TPS)—indicative of contraction duration, time to 90% relenghthening (TR90)—representing cardiomyocyte relaxation duration, and maximal velocities of shortening ($+dL/dt$) and relenghthening ($-dL/dt$)—indicators of maximal velocities of ventricular pressure rise/fall. Myocytes were loaded with Fura-2AM (0.5 μM) for 10 min and fluorescence measurements were recorded. Resting calcium, qualitative changes in the intracellular calcium, and fluorescence decay time (Tau) were measured. Both single- and biexponential curve-fit programs were applied to calculate the intracellular Ca^{2+} decay constant [3,30]. At least 25 individual cardiomyocytes isolated from 3 to 5 Wistar rats were used for data collection. Changes in $[Ca]_i$ were calculated by determining the rise in $[Ca]_i$ relative to basal levels measured

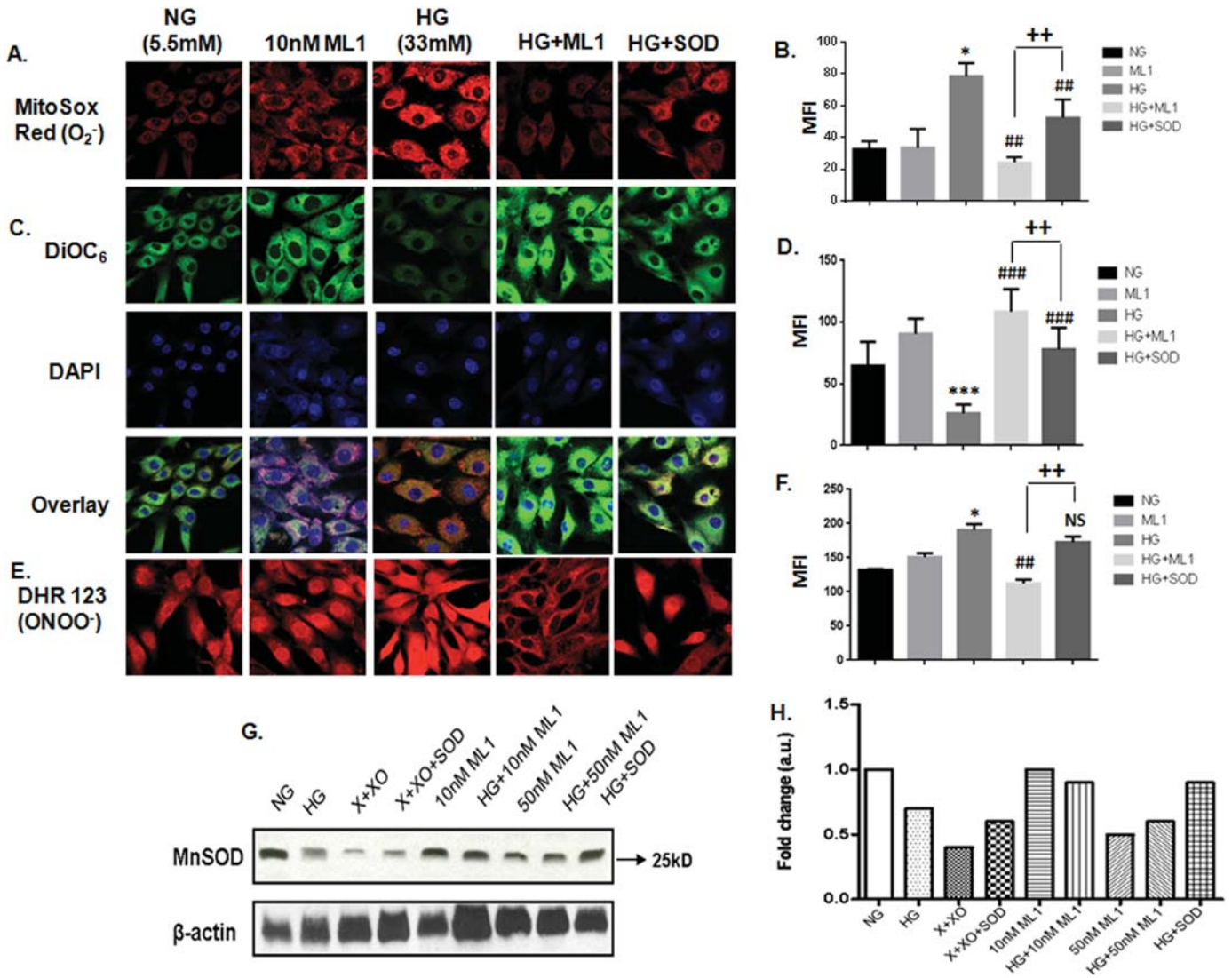

Fig. 2. ML1 restores mitochondrial function via upregulation of Mn-SOD. (A) Mitochondrial superoxide production was quantified using Mitosox™ red. (C) Mitochondrial membrane potential was determined using $DiOC_6$. (E) Peroxynitrite production was assessed using DHR-123. (B, D, F) Fluorescence intensity profiles were quantified using Image J software for above mentioned experiments. Columns, mean from three independent experiments performed in triplicate; bars, SE. $^{*}P < 0.05$, $^{***}P < 0.001$ versus NG and $^{\#\#}P < 0.01$, $^{\#\#\#}P < 0.001$ versus HG, $^{++}P < 0.01$ versus HG+SOD. (G, H) Mn-SOD expression was studied using western blotting and quantified using Image J software. Image representative of three independent experiments and fold change plotted according to represented blot. Statistical analysis was performed using student's *t* test.

immediately before that particular experimental maneuver.

2.10. Statistical analysis

All experiments were performed at least three times for each determination. Data are expressed as means ± standard error (SE) and were analyzed using one-way analysis of variance using Tukeys post hoc correction and secondary analysis for significance was carried out with Student's *t* test using Prism 4.0 GraphPad software (GraphPad, San Diego, CA, USA). Differences were considered to be significant at $P < 0.05$.

3. Results

3.1. The Cytoprotective effect of ML1 in H9c2 line.

In order to study the cardio-protection of ML1 against high glucose, we used a rat cardiac myoblast H9c2 cell line. ML1 when given alone at concentrations of 10, 50, 100 nM (without HG) did not show any toxicity, as shown in Fig. 1A. The mitochondrial Mn-SOD (100U), which served as a positive control, could not prevent HG-induced H9c2 cell death, however all the concentrations of ML1 significantly abrogated HG induced cytotoxicity (Fig. 1A). To determine whether the observed cytoprotective effects of ML1 was a measure of its anti-oxidant potential, we incubated these cells with an exogenous O_2^-, generator Xanthine+Xanthine Oxidase (X+XO). Interestingly, ML1 also inhibited cell death induced by the X+XO, but the effect was more pronounced at lower concentrations of ML1 (10 nM) and was less effective at higher concentrations (Fig. 1B).The protective effect of ML1 on HG-induced cell viability in H9c2 cells was further demonstrated by inhibition of PARP cleavage. As shown in Fig. 1C, pretreatment with ML1 (10 and 50 nM) significantly reduced PARP cleavage induced by HG in H9c2 cells. However, SOD (100U), which served as a positive control, did not prevent PARP cleavage at this concentration.

3.2. The effect of ML1 on mitochondrial superoxide (O_2^-) and peroxynitrite production and Mn-SOD expression

Although not a strong oxidant itself, O_2^-, the product of a one-electron reduction of oxygen, is the precursor of most ROS and a

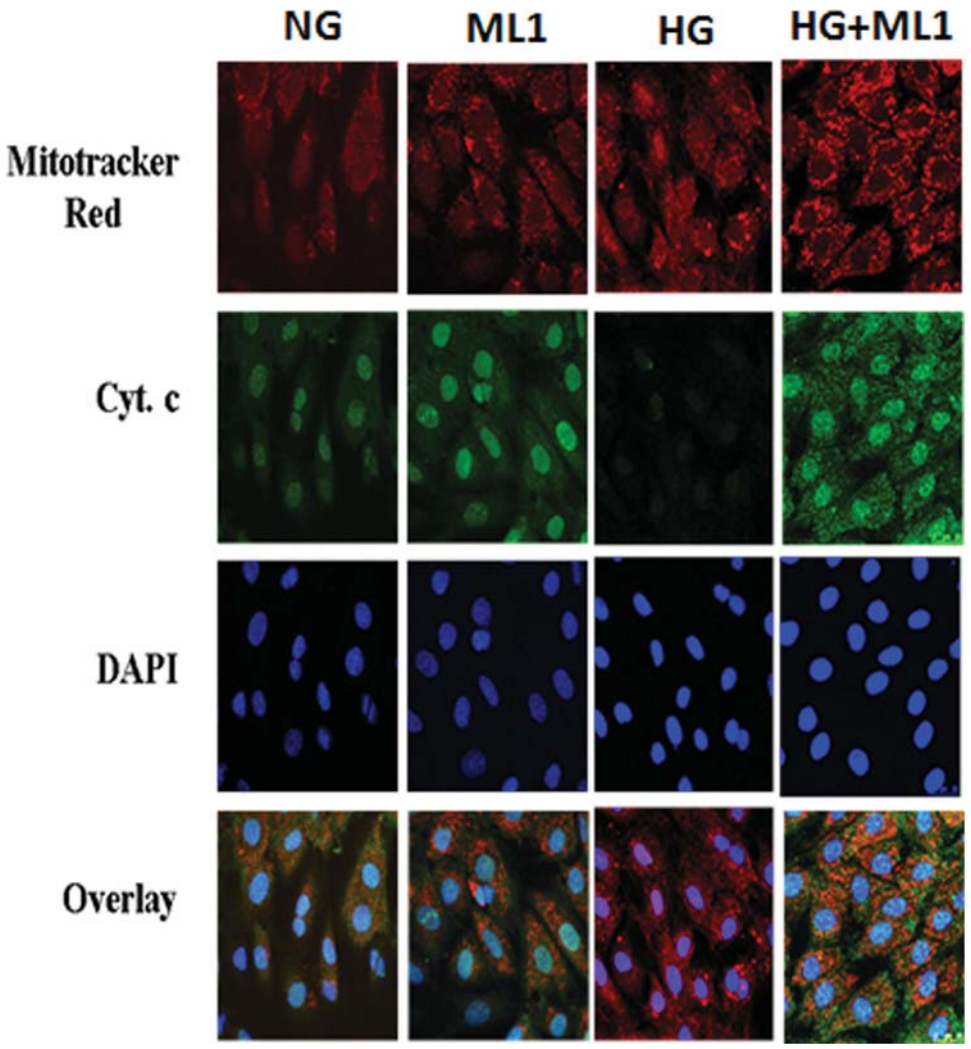

Fig. 3. ML1 prevents cytochrome c release. Cytochrome c release was observed by confocal microscopy. Mitochondria were labeled using Mitotracker red, cytochrome c antibody was detected using Cy2-conjugated goat anti-rabbit secondary antibody and nuclei were counterstained using DAPI. Image representative of three independent experiments.

mediator in oxidative chain reactions [31]. If not scavenged properly, $O_2^{\cdot-}$ may react with NO and generate a very powerful and toxic oxidant, peroxynitrite ($ONOO^-$) [32,33]. Therefore, we determined the intracellular levels of mitochondrial $O_2^{\cdot-}$ using Mitosox™ red and peroxynitrite using DHR 123. Fig. 2 demonstrated that when administrated prior (2 h) to HG treatment for 48 h, ML1 (10 nM) suppressed mitochondrial $O_2^{\cdot-}$ generation (Fig. 2A and B) and peroxynitrite generation (Fig. 2E and F) in HG-treated H9c2 cells, indicating a putative antioxidant property of the SOD mimic. Since an increase in mitochondrial ROS generation leads to a decrease in mitochondrial membrane potential, we further evaluated the efficiency of ML-1 in restoring HG-induced mitochondrial depolarization in H9c2 cells. The molecular probe $DiOC_6$ was used to assess mitochondrial membrane depolarization. $DiOC_6$ is a mitochondria specific fluorescent dye and is widely used in monitoring $\Delta\Psi_m$ because it offers the important advantage that it does not show major quenching effects [34,35]. As shown in Fig. 2.C and D, treatment with HG leaded to a decrease in fluorescence intensity indicating loss of $\Delta\Psi_m$. Pretreatment with ML1 restored the loss of mitochondrial membrane potential in cells exposed to HG. Interestingly, ML1 afforded comparatively better protection than SOD with respect to the aforementioned measures of HG induced oxidative stress (Fig. 2 B, D and F). Further investigation into the anti-oxidative mechanism of ML1 demonstrated that HG-induced a decrease in the expression of Mn-SOD, one of the major and precursor antioxidant enzymes, capable of dismutating $O_2^{\cdot-}$, into H_2O_2. This was attenuated by pretreatment with ML1 (10 nM) (Fig. 2G and H). No effect was seen when ML1 was given alone (without HG). These findings indicate that ML1 decreases HG-induced mitochondrial $O_2^{\cdot-}$ and $ONOO^-$ partly through up-regulation of Mn-SOD activity. These results suggest that the antioxidant enzyme Mn-SOD plays an important role in the anti-apoptotic action of ML1 against HG-induced damage.

3.3. *ML1 attenuated HG-induced cytochrome c release.*

It is well known that mitochondria play a pivotal role in cell death/ survival and that mitochondrial dysfunction constitutes a critical event in the apoptotic process. $\Delta\Psi_m$ is a critical factor in maintaining the integrity of mitochondria and subsequent regulation of apoptosis. Loss of $\Delta\Psi_m$ will lead to release of cytochrome c from mitochondria, which in turn activates downstream caspases and causes PARP cleavage, an endogenous caspase substrate to cause apoptosis [36,37]. Thus we evaluated the effect of ML1 on HG-induced cytochrome c release from mitochondria. In the untreated cells, cytochrome c co-localized in the mitochondria (Fig. 3), however after exposure of H9c2 cells to HG, cytochrome c was observed to have diffused out from the mitochondria at 72 h. This HG induced release of cytochrome c was attenuated by ML1.

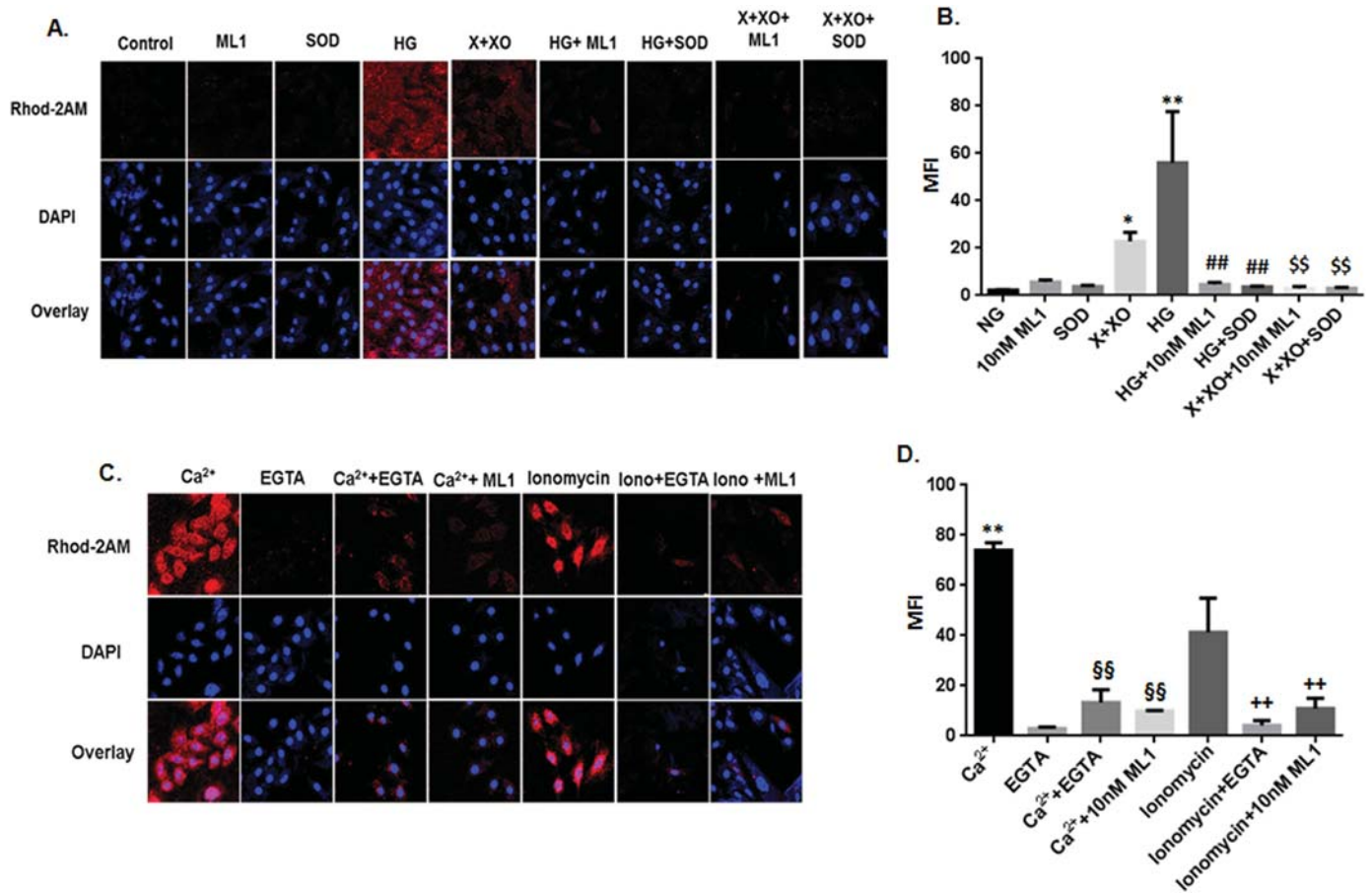

Fig. 4. ML1 inhibited HG-induced mitochondrial calcium overload. (A) Protection by ML1 against HG induced mitochondrial calcium was evaluated using Rhod-2AM. (B) Mean fluorescence intensity (MFI) was analyzed using image J software. (C) Ability of ML1 to counter external calcium induction was assessed using Rhod-2 AM. (D) Mean fluorescence intensity (MFI) was analyzed using image J software. Image representative of three independent experiments. Columns, mean from three independent experiments performed in triplicate; bars, SE. $^{*}P<0.05$, $^{**}P<0.01$ versus NG, $^{\#\#}P<0.01$ versus HG, $^{\$\$}P<0.01$ versus X+XO, $^{\S\S\S}P<0.001$ versus calcium and $^{++}P<0.01$ versus ionomycin.

3.4. ML1 inhibited HG-induced mitochondrial calcium overload

As shown in previous studies, high glucose conditions lead to an increase in mitochondrial calcium overload which is one of the main pathological stimuli for the induction of diabetic cardiomyopathy [23]. An increase in intracellular calcium is implicated in elevating mitochondrial ROS levels and further reducing membrane potential, thus facilitating the release of apoptogenic cytochrome c [38–41], ultimately providing the premise for ischemic heart disease. Therefore, to examine whether the mitochondrial calcium overload can be ameliorated by the protective effect of ML1 on HG-induced apoptosis, the molecular probe Rhod-2AM was used to assess mitochondrial calcium accumulation. Treatment with HG leads to an increase in the fluorescence levels, indicative of accumulation of Ca^{2+} into the mitochondria. This could be inhibited by pretreatment with ML1 as well as SOD (Fig. 4A and B). The exogenous O_2^-, generator X+XO also increased Rhod-2 fluorescence, but to a relatively low extent. Both SOD and ML1 abolished the rise in Rhod-2 fluorescence completely (Fig. 4A, B). Calcium chloride ($CaCl_2$) and the Ca^{2+} mobilizing compound, ionomycin used as positive controls for mitochondrial calcium overload [42–45] also lead to an increase in mitochondrial Ca^{2+} accumulation which was inhibited by both the calcium chelator EGTA as well as ML1 (Fig. 4C and D).

3.5. ML1 protects against high-glucose-induced abnormalities in relaxation in rat ventricular myocytes

Culturing myocytes for 24 h with either HG or ML1 had no overt effect on cell phenotype. Cell shape, resting cell length, and presence of distinct striations were similar in cells among the two groups. Representative traces of cell shortening and relengthening are shown in Fig. 5A. Consistent with previous reports [5,45–47], myocytes maintained in high-glucose medium had a reduced peak shortening amplitude (Fig. 5B) associated with decreased maximal velocity of shortening and relenghthening ($\pm$dL/dt) (Fig. 5A), elevated time-to-peak shortening (TPS) (Fig. 5C), and prolonged time to- 90% relenghthening (TR90) (Fig. 5D) compared to those of normal myocytes. The reduced peak shortening, $\pm$dL/dt, elevated TPS and prolonged TR90 in HG myocytes were abolished by co-incubation of the cells with 10 nM ML1 (Fig. 5B–D).

3.6. Effect of ML1 on intracellular Ca^{2+} ($[Ca^{2+}]_i$) transients

To determine whether the differential response of ML1 in NG and HG cultured ventricular myocytes was due to changes in intracellular Ca^{2+} concentration, we used the fluorescent dye fura-2 to estimate intracellular Ca^{2+} transient properties in myocytes from both groups. Earlier studies have also shown that prolonged relaxation in HG-treated cells is accompanied by slower intracellular Ca^{2+} clearing [45,46,48]. Since ML1 prevented HG-induced relaxation dysfunctions, we wanted to determine whether this effect coincided with changes in intracellular Ca^{2+}. Resting $[Ca^{2+}]$i, electrical stimulus-induced increase in intracellular Ca^{2+} ($\Delta[Ca^{2+}]$i), and cytosolic free Ca^{2+} decrease rate (tau) were evaluated in fura-2 loaded myocytes. HG myocytes showed similar

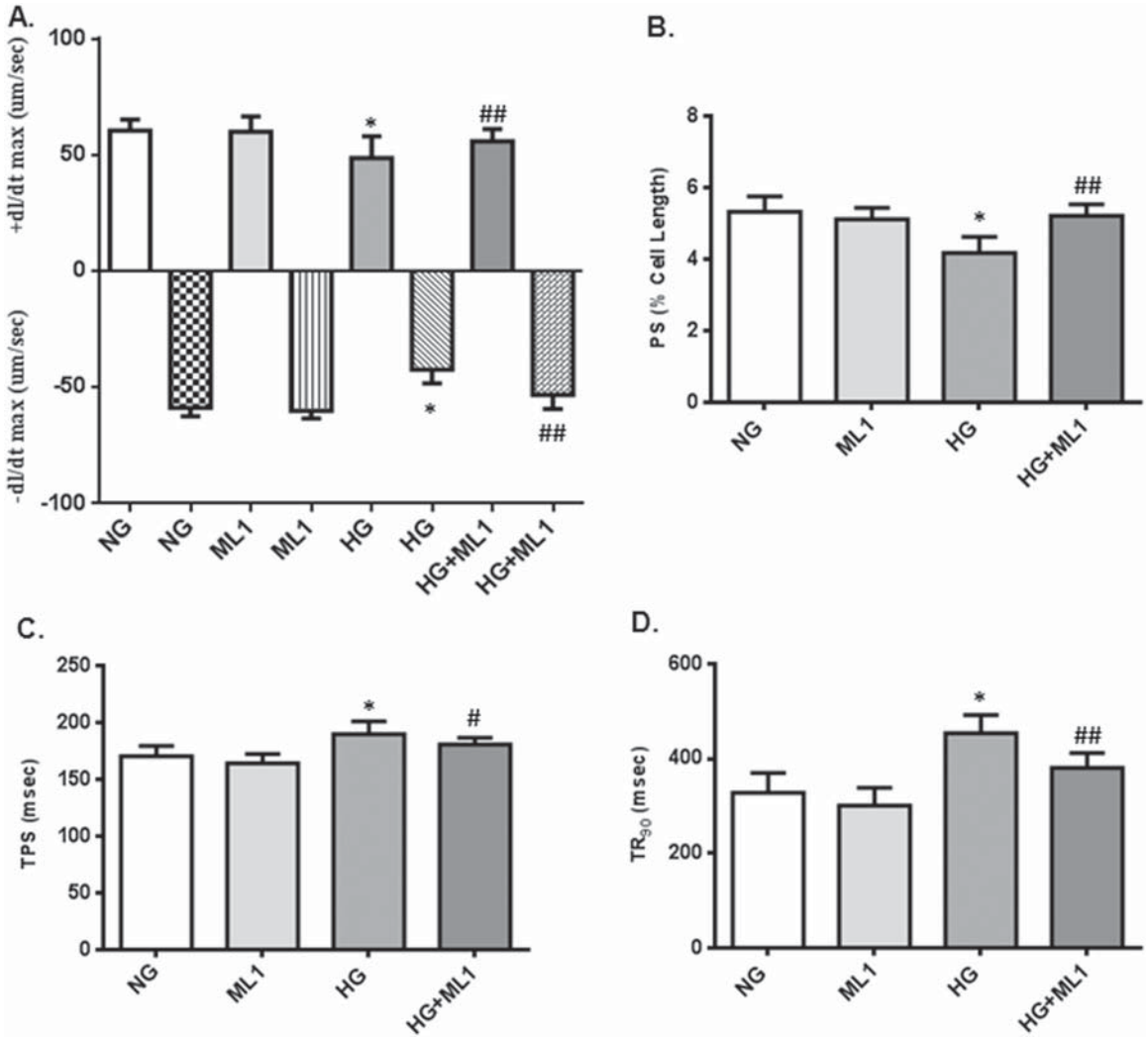

Fig. 5. ML1 rescues ARVMs from high-glucose-induced abnormalities in relaxation. High glucose induced (A) shortening and re-lengthening (± dL/dt) (B) peak shortening amplitude (C) time-to-peak shortening (TPS) and (D) time to- 90% re-lengthening (TR90) were studied using a SoftEdge MyoCam system. Columns, mean from three independent experiments performed in triplicate; bars, SE. $^{*}P < 0.05$ versus NG, $^{\#}P < 0.05$, $^{\#\#}P < 0.01$ versus HG.

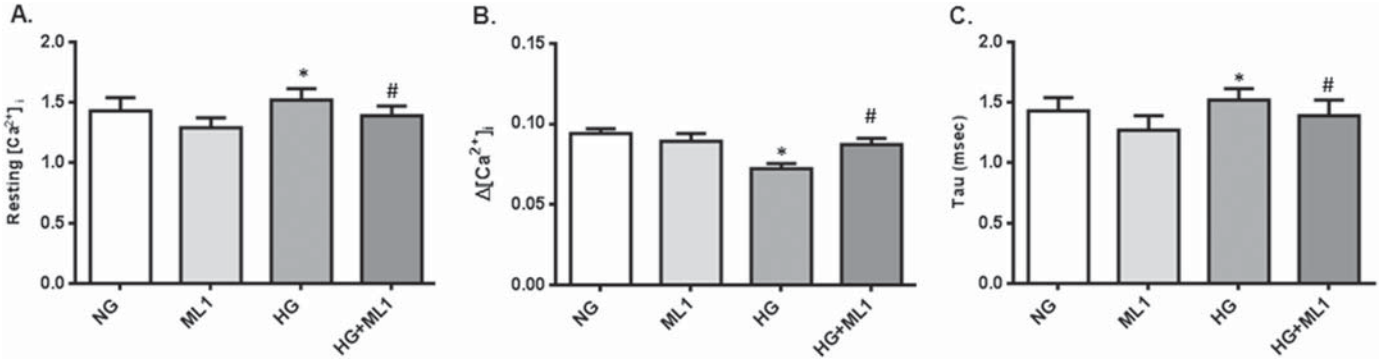

Fig. 6. ML1 modulates intracellular calcium transients. High glucose mediated changes in (A) resting $[Ca^{2+}]$I, (B) intracellular calcium $\Delta[Ca^{2+}]$i and (C) cytosolic-free Ca^{2+} release rate, Tau were detected using a SoftEdge MyoCam system. Columns, mean from three independent experiments performed in triplicate; bars, SE. $^{*}P < 0.05$ versus NG, $^{\#}P < 0.05$ versus HG.

resting $[Ca^{2+}]$i (Fig. 6A), reduced $\Delta[Ca^{2+}]$i (Fig. 6B) associated with slower cytosolic-free Ca^{2+} (Fig. 6C) decrease compared to normal myocytes, consistent with reduced peak shortening and prolonged TR90. ML1 (10 nM) abolished the HG-induced reduction of $\Delta[Ca^{2+}]$i and prolonged cytosolic free Ca^{2+} decrease (Fig. 6B and C).

4. Discussion

In this work, we show that ML-1, a novel SOD mimic with a redox-modulating Mn (II) complex inhibits mitochondrial dysfunction in H9c2 cells, in which it prevents ROS and hyperglycemia-induced cell death. It also rescues HG-induced abnormalities

in myocyte relaxation, in an ex-vivo ARVM model. We propose that the protective effect of ML1 manifests through its antioxidant potential, and might be responsible for stalling HG stress induced apoptotic events.

As reported in our previous study [22], ML1 appears to exert superior protection against oxidative damage in Hek293 kidney cells, as compared with Mn-SOD, used here as a positive control. In the present study, H9c2 cells exposed to 33 mM of glucose decreased cell viability while pre-treatment with ML1 restored cell viability. The results of this MTT assay are based mainly on the enzymatic conversion of MTT within the mitochondria by succinate dehydrogenase, which suggests that the early signs of glucose toxicity could be based on mitochondrial dysfunction. This indicates that the mitochondrion-driven apoptotic pathway is closely linked to glucose metabolism. The protective effect of ML1 was further confirmed by its inhibition of HG and X+XO induced PARP cleavage, an event associated with DNA damage and cell death. The fact that Mn-SOD was able to inhibit PARP cleavage due to X+XO induced cytotoxicityand was ineffective against High glucose stress, indicates that Mn-SOD is able to counter only acute ROS production by X+XO, whereas ML-1 can inhibit both the acute and, HG mediated chronic toxicity. The harmful effects of ROS on cells is widely appreciated, and findings from our previous studies [22] as well in the current study confirm that exogenous oxidizing agent X+XO alters cell viability irrespective of the cell type. This implies that the adverse effects of hyperglycemia in cultured cardiac cells are at least partly attributable to the occurrence of an oxidative stress. The fact that ML1 prevents X+XO induced cell death in H9c2 cells suggests that ML1 may affect an event that follows ROS generation.

Calcium overload and oxidative insult are the two mutually non-exclusive phenomena suggested to cause cardiac dysfunction. The involvement of oxidative and/or nitrosative stress [1,23] and an alteration in calcium homeostasis due to Ca^{2+} overload [23,49] in the pathogenesis of diabetic cardiomyopathy has been implicated in experimental animal studies and in patients. The overproduction of superoxide and its associated peroxynitrite have been recognized as an important contributor to diabetic vascular complications [6,7]. Oxidative stress, induced by reactive oxygen and nitrogen species derived from hyperglycemia, causes abnormal gene expression, altered signal transduction, and the activation of pathways leading to programmed myocardial cell death. This is evident from our studies, where exposure of H9c2 cells to HG leads to increased $O_2^{\cdot-}$ and $ONOO^-$ levels. An upregulation of Mn-SOD levels along with an effective quenching of free radicals provides further proof of the anti-oxidant potential of ML1.

Among various effects of ROS on cell metabolism, reduction in mitochondrial membrane potential ($\Delta\Psi_m$) which is the rate limiting manifestation of mitochondrial cell death is of crucial importance [50]. The fact that HG-induced oxidative stress reduced mitochondrial membrane potential, facilitated cytochrome *c* release and PARP cleavage, whereas ML1 prevented all of these events, strongly suggests that oxidative stress induced cytotoxicity in cardiac cells is mainly due to mitochondrial dysfunction. ML1restored mitochondrial membrane potential and blocked the release of cytochrome *c,* probably by neutralizing ROS and RNS toxicity. This property was found to be superior to exogenously added SOD, hinting at the cellular permeability of ML1.

The reason for inhibition of mitochondrial Ca^{2+} over load in HG treated cells by ML1 could be attributed to inhibition of excessive ROS production, however, it could also relate to its inhibition of mitochondrial ATP-sensitive potassium channel ($mitoK_{ATP}$) channels, since studies in cardiac myocytes have shown that $mitoK_{ATP}$ is activated by superoxide and hydrogen peroxide and is regulated in a redox-dependent manner by reactive nitrogen species [51]. This channel may also facilitate ROS-mediated cell death in high glucose treated cardiac cells, possibly by acting as an uncoupling agent that decreases membrane potential and mitochondrial calcium overload, as in the case of ischemic preconditioning [52] although the precise mechanism remains unclear.

Further, we took advantage of a cardiac myocyte culture model developed in our laboratory, where diabetic cardiomyopathy could be phenotypically replicated in normal myocytes by culturing in a high glucose medium. It has been well established that high glucose impairs cardiac E-C coupling and induces contractile dysfunctions in isolated cardiomyocytes [5,46,48]. The abnormal cardiac E-C coupling is apparent in high glucose-treated myocytes reminiscent of those from in vivo diabetes [4]. The freshly isolated myocytes from diabetic rats, and normal myocytes cultured in HG-containing medium, exhibit prolonged relaxation and slowed cytosolic Ca^{2+} removal [4,46,48]. Prolonged relaxation associated with slow intracellular Ca^{2+}extrusion is the most consistent feature in diabetic cardiomyopathy as inferred from previous experiments [5,7,28,53]. In the current study, ML1 improved HG-induced relaxation dysfunction without affecting mechanical indices in normal cells. This effect is associated with the improvement of cytosolic Ca^{2+} clearing, which may underlie ML1 activity. Elevated extracellular glucose leads to increased intracellular Ca^{2+} in both vascular smooth muscle [5] and cardiomyocytes [49,54], which may be responsible for altered E-C coupling. These alterations may cause changes in intracellular Ca^{2+} homeostasis and, in turn, the cardiac defects [55]. We measured calcium transients in diabetic rat myocytes and demonstrated a decrease in both the peak amplitude and the rate of decay of calcium transients, suggesting a depression in SR calcium handling.

In summary, this study underlines the important role of mitochondrial superoxide overproduction and calcium overload in diabetic cardiomyopathy and indicates that treatment with low molecular weight SOD mimetics can be beneficial in preserving cardiac contractility in this disease. Our study suggests that ML1 could be a potential therapeutic agent for diabetic cardiac disorders and other disorders that involve oxidative stress associated with mitochondrial injury. However, a much more detailed study delineating its mechanism of action would reveal valuable targets for novel therapeutics aimed at preventing diabetes related cardiac diseases including DCM more efficiently.

Acknowledgment

We thank Dr. S. C. Mande, Director, National Centre for Cell Science (Pune, India) for encouragement and support.

This work was supported by the National Centre for Cell Science, Department of Biotechnology, India. A.D. (Sr. No. 1060931113), M A.S (Sr. No.1060931147), are recipients of Council for Scientific and Industrial Research Fellowships.

Appendix A. Transparency Document

Transparency Document associated with this article can be found in the online version at http://dx.doi.org/10.1016/j.bbrep.2016.01.003.

References

[1] L. Cai 1, W. Li, G. Wang, L. Guo, Y. Jiang, Y.J. Kang, Hyperglycemia-induced apoptosis in mouse myocardium: mitochondrial cytochrome C-mediated caspase-3 activation pathway, Diabetes 51 (6) (2002) 1938–1948.

[2] S. Kumar, S. Prasad, S.L. Sitasawad, Multiple antioxidants improve cardiac complications and inhibit cardiac cell death in streptozotocin-induced diabetic rats, PLoS One 8 (7) (2013) e67009.

[3] V. Kain, S. Kumar, S.L. Sitasawad, Azelnidipine prevents cardiac dysfunction in streptozotocin-diabetic rats by reducing intracellular calcium accumulation, oxidative stress and apoptosis, Cardiovasc. Diabetol. 10 (2011) 97.
[4] J. Ren, A.J. Davidoff, Diabetes rapidly induces contractile dysfunctions in isolated ventricular myocytes, Am. J. Physiol. 272 (1 Pt 2) (1997) H148–H158.
[5] J. Ren, L.J. Dominguez, J.R. Sowers, A.J. Davidoff, Troglitazone attenuates high-glucose-induced abnormalities in relaxation and intracellular calcium in rat ventricular myocytes, Diabetes 45 (12) (1996) 1822–1825.
[6] L. Cai 1, J. Wang, Y. Li, X. Sun, L. Wang, Z. Zhou, Y.J. Kang, Inhibition of superoxide generation and associated nitrosative damage is involved in metallothionein prevention of diabetic cardiomyopathy, Diabetes 54 (6) (2005) 1829–1837.
[7] Cai L 1, Y.J. Kang, Oxidative stress and diabetic cardiomyopathy: a brief review, Cardiovasc. Toxicol. 1 (3) (2001) 181–193.
[8] X. Shen 1, S. Zheng, N.S. Metreveli, P.N. Epstein, Protection of cardiac mitochondria by overexpression of MnSOD reduces diabetic cardiomyopathy, Diabetes 55 (3) (2006) 798–805.
[9] M.A. Yorek, D. Beebe, P.J. Oates, H.P. Hammes, I. Giardino, M. Brownlee, Normalizing mitochondrial superoxide production blocks three pathways of hyperglycaemic damage, Nature 404 (2000) 787–790.
[10] X. Shen, S. Zheng, V. Thongboonkerd, M. Xu, W.M. Pierce Jr, J.B. Klein, P. N. Epstein, Cardiac mitochondrial damage and biogenesis in a chronic model of type 1 diabetes, Am. J. Physiol. Endocrinol. Metab 287 (2004) E896–E905.
[11] S. Medikayala, B. Piteo, X. Zhao, J.G. Edwards, Chronically elevated glucose compromises myocardial mitochondrial DNA integrity by alteration of mitochondrial topoisomerase function, Am. J. Physiol. Cell. Physiol. 300 (2) (2011) C338–C348.
[12] P. Umbarkar, S. Singh, S. Arkat, S.L. Bodhankar, S. Lohidasan, S.L. Sitasawad, Monoamine oxidase-A (MAO-A) is an important source of oxidative stress and promotes cardiac dysfunction, apoptosis, and fibrosis in diabetic cardiomyopathy, Free Radic. Biol. Med. 87 (2015) 263–273, pii: S0891-5849(15)00293-2.
[13] L. Benov, I. Batini´c-Haberle, A manganese porphyrin suppresses oxidative stress and extends the life span of streptozotocin diabetic rats, Free Radic. Res. 38 (2005) 81.
[14] C. Levrand, B. Vannay-Bouchiche, P. Pesse, F. Pacher, B. Feihl, Waeber, L. Liaudet, Peroxynitrite is a major trigger of cardiomyocyte apoptosis in vitro and in vivo, Free Radic. Biol. Med. 41 (2006) 886–895.
[15] N. Hayakawa, S. Asayama, Y. Noda, T. Shimizu, H. Kawakami, Pharmaceutical effect of manganese porphyrins on manganese superoxide dismutase deficient mice, Mol. Pharm. 9 (10) (2012) 2956–2959.
[16] J.P. Crow 1, N.Y. Calingasan, J. Chen, J.L. Hill, M.F. Beal, Manganese porphyrin given at symptom onset markedly extends survival of ALS mice, Ann. Neurol. 58 (2) (2005) 258–265.
[17] S. Dogan 1, M. Unal, N. Ozturk, P. Yargicoglu, Cort A. Spasojevic I, I. Batinic-Haberle, M. Aslan, Manganese porphyrin reduces retinal injury induced by ocular hypertension in rats, Exp. Eye Res. 93 (4) (2011) 387–396.
[18] L.P. Liang, S. Waldbaum, S. Rowley, T.T. Huang, B.J. Day, M. Patel, Mitochondrial oxidative stress and epilepsy in SOD2 deficient mice: attenuation by a lipophilic metalloporphyrin, Neurobiol. Dis. 45 (3) (2012) 1068–1076.
[19] C. Cruz, J. Koepp, I. Batinic-Haberle, J. Crapo, B. Day, R. Kachadourian, R. Young, B. Bradley, K. Haskins, A metalloporphyrin-based superoxide dismutase mimic inhibits adoptive transfer of autoimmune diabetes by a diabetogenic T-cell clone. Piganelli JD1, Flores SC, Diabetes 51 (2) (2002) 347–355.
[20] S. Miriyala 1, Spasojevic I, A. Tovmasyan, D. Salvemini, Z. Vujaskovic, D. St Clair, I. Batinic-Haberle, Manganese superoxide dismutase, MnSOD and its mimics, Biochim. Biophys. Acta 1822 (5) (2012) 794–814.
[21] I. Batinić-Haberle, J.S. Rebouças, I. Spasojević, Superoxide dismutase mimics: chemistry, pharmacology, and therapeutic potential, Antioxid. Redox Signal. 13 (6) (2010) 877–918.
[22] A. Vyas, V. Kain, Z. Afrasiabi, S. Sitasawad, M. Khetmalas, V. Nivière, S. Padhye, Novel Mn-SOD mimetics offer superior protection against oxidative damages in Hek293 kidney cells, J. Pharm. Sci. Pharmacol. 1 (2014) 146–153.
[23] S. Kumar, V. Kain, S.L. Sitasawad, High glucose-induced Ca^{2+} overload and oxidative stress contribute to apoptosis of cardiac cells through mitochondrial dependent and independent pathways, Biochim. Biophys. Acta 1820 (7) (2012) 907–920.
[24] T.L. Broderick 1, G. Haloftis, D.J. Paulson, l-propionylcarnitine enhancement of substrate oxidation and mitochondrial respiration in the diabetic rat heart, J. Mol. Cell. Cardiol. 28 (2) (1996) 331–340.
[25] A. Vanella, A. Russo, R. Acquaviva, A. Campisi, C. Di Giacomo, V. Sorrenti, M. L. Barcellona, L -propionyl-carnitine as superoxide scavenger, antioxidant, and DNA cleavage protector, Cell Biol. Toxicol. 16 (2) (2000) 99–104.
[26] C. Felix 1, M. Gillis, W.R. Driedzic, D.J. Paulson, T.L. Broderick, Effects of propionyl-l-carnitine on isolated mitochondrial function in the reperfused diabetic rat heart, Diabetes Res. Clin. Pract. 53 (1) (2001) 17–24.
[27] Cameron N.E. Cotter MA1, A. Keegan, K.C. Dines, Effects of acetyl- and propionyl-l-carnitine on peripheral nerve function and vascular supply in experimental diabetes, Metabolism 44 (9) (1995) 1209–1214.
[28] P. Murugavel, L. Pari, S.L. Sitasawad, S. Kumar, S. Kumar, Cadmium induced mitochondrial injury and apoptosis in vero cells: protective effect of diallyl tetrasufide from garlic, Int. J. Biochem. Cell. Biol. 39 (1) (2007) 161–170.
[29] Kim H.S. Youn HJ1, M.H. Jeon, J.H. Lee, Y.J. Seo, Y.J. Lee, J.H. Lee, Induction of caspase-independent apoptosis in H9c2 cardiomyocytes by adriamycin treatment, Mol. Cell. Biochem. 270 (1–2) (2005) 13–19.
[30] J. Ren, L.E. Wold, Measurement of Cardiac Mechanical Function in Isolated Ventricular Myocytes from Rats and Mice by Computerized Video-Based Imaging, Biol. Proced. Online 11 (3) (2001) 43–53.
[31] J.F. Turrens 1, Mitochondrial formation of reactive oxygen species, J. Physiol. 552 (Pt 2) (2003) 335–344.
[32] J.S. Beckman, W.H. Koppenol, Nitric oxide, superoxide, and peroxynitrite: the good, the bad, and ugly, Am. J. Physiol. 271 (5 Pt 1) (1996) C1424–C1437.
[33] R. Radi 1, A. Cassina, R. Hodara, C. Quijano, L. Castro, Peroxynitrite reactions and formation in mitochondria, Free Radic. Biol. Med. 33 (11) (2002) 1451–1464.
[34] M. Castedo 1, K. Ferri, T. Roumier, D. Métivier, N. Zamzami, G. Kroemer, Quantitation of mitochondrial alterations associated with apoptosis, J. Immunol. Methods 265 (1–2) (2002) 39–47.
[35] P. Bernardi, L. Scorrano, R. Colonna, V. Petronilli, F. Di Lisa, Mitochondria and cell death. Mechanistic aspects and methodological issues, Eur. J. Biochem. 264 (3) (1999) 687–701.
[36] M. Crompton, Mitochondrial intermembrane junctional complexes and their role in cell death, J. Physiol. 529 (Pt 1) (2000) 11–21.
[37] P. Newsholme 1, E.P. Haber, S.M. Hirabara, E.L., Procopio J. Rebelato, D. Morgan, H.C. Oliveira-Emilio, A.R. Carpinelli, R. Curi, Diabetes associated cell stress and dysfunction: role of mitochondrial and non-mitochondrial ROS production and activity, J. Physiol. 583 (Pt 1) (2007) 9–24.
[38] D. Gincel 1, H. Zaid, V. Shoshan-Barmatz, Calcium binding and translocation by the voltage-dependent anion channel: a possible regulatory mechanism in mitochondrial function, Biochem. J. 358 (Pt 1) (2001) 147–155.
[39] T. Hodge 1, M. Colombini, Regulation of metabolite flux through voltage-gating of VDAC channels, J. Membr. Biol. 157 (3) (1997) 271–279.
[40] A.P. Halestrap, G.P. McStay, S.J. Clarke, The permeability transition pore complex: another view, Biochimie. 84 (2–3) (2002) 153–166.
[41] R. Foyouzi-Youssefi 1, S. Arnaudeau, C. Borner, W.L. Kelley, J. Tschopp, D.P. Lew, N. Demaurex, K.H. Krause, Bcl-2 decreases the free Ca^{2+} concentration within the endoplasmic reticulum, Proc. Natl. Acad. Sci. USA 97 (11) (2000) 5723–5728.
[42] Miller A.C. Squìer MK1, A.M. Malkinson, J.J. Cohen, Calpain activation in apoptosis, J. Cell. Physiol. 159 (2) (1994) 229–237.
[43] C. Widmann, S. Gibson, G.L. Johnson, Caspase-dependent cleavage of signaling proteins during apoptosis. A turn-off mechanism for anti-apoptotic signals, J. Biol. Chem. 273 (12) (1998) 7141–7147.
[44] J. Lotem 1, R. Kama, L. Sachs, Suppression or induction of apoptosis by opposing pathways downstream from calcium-activated calcineurin, Proc. Natl. Acad. Sci. USA 96 (21) (1999) 12016–12020.
[45] Y. Chvatchko 1, S. Valera, J.P. Aubry, T. Renno, G. Buell, J.Y. Bonnefoy, The involvement of an ATP-gated ion channel, P(2X1), in thymocyte apoptosis, Immunity 5 (3) (1996) 275–283.
[46] J. Ren, G.A. Gintant, R.E. Miller, A.J. Davidoff, High extracellular glucose impairs cardiac E-C coupling in a glycosylation-dependent manner, Am. J. Physiol. 273 (6 Pt 2) (1997) H2876–H2883.
[47] J. Ren, J. Duan, K.K. Hintz, B.H. Ren, High glucose induces cardiac insulin-like growth factor I resistance in ventricular myocytes: role of Akt and ERK activation, Cardiovasc. Res. 57 (3) (2003) 738–748.
[48] A.J. Davidoff, J. Ren, Low insulin and high glucose induce abnormal relaxation in cultured adult rat ventricular myocytes, Am. J. Physiol. 272 (1 Pt 2) (1997) H159–H167.
[49] M. Smogorzewski 1, Galfayan V, S.G. Massry, High glucose concentration causes a rise in [Ca^{2+}]i of cardiac myocytes, Kidney Int. 53 (5) (1998) 1237–1243.
[50] M.A. Aon, S. Cortassa, B. O'Rourke, Redox-optimized ROS balance: a unifying hypothesis, Biochim. Biophys. Acta 1797 (2010) 865–877.
[51] B.B. Queliconi, A.P. Wojtovich, S.M. Nadtochiy, A.J. Kowaltowski, P.S. Brookes, Redox regulation of the mitochondrial K(ATP) channel in cardioprotection, Biochim. Biophys. Acta 1813 (2011) 1309–1315.
[52] A.M. Walters, G.A. Porter Jr., P.S. Brookes, Mitochondria as a drug target in ischemic heart disease and cardiomyopathy, Circ. Res. 111 (2012) 1222–1236.
[53] D.L. Lagadic-Gossmann, K.J. Buckler, K. Le Prigent, D. Feuvray, Altered Ca^{2+} handling in ventricular myocytes isolated from diabetic rats, Am. J. Physiol. 270 (1996) H1529–H1537.
[54] R.K. Gupta, B.A. Wittenberg, 1 9F nuclear magnetic resonance studies of free calcium in heart cells, Biophys. J. 65 (1993) 2547–2558.
[55] W.H. Barry, J.H.B. Bridge, Intracellular calcium homeostasis in cardiac myocytes, Circulation 87 (1993) 1806–1815.